

University of Wollongong

## Research Online

---

Australian Institute for Innovative Materials -  
Papers

Australian Institute for Innovative Materials

---

1-1-2009

### Fabrication and superconducting properties of highly dense MgB<sub>2</sub> bulk using a two-step sintering method

Minoru Maeda

*University of Wollongong*

Yue Zhao

*University of Wollongong, [yue\\_zhao@uow.edu.au](mailto:yue_zhao@uow.edu.au)*

Yoshifumi Watanabe

*Nihon University, Japan*

Hiroaki Matsuoka

*Nihon University, Japan*

Y Kubota

*Nihon University, Japan*

Follow this and additional works at: <https://ro.uow.edu.au/aiimpapers>



Part of the [Engineering Commons](#), and the [Physical Sciences and Mathematics Commons](#)

---

#### Recommended Citation

Maeda, Minoru; Zhao, Yue; Watanabe, Yoshifumi; Matsuoka, Hiroaki; and Kubota, Y, "Fabrication and superconducting properties of highly dense MgB<sub>2</sub> bulk using a two-step sintering method" (2009).

*Australian Institute for Innovative Materials - Papers*. 54.

<https://ro.uow.edu.au/aiimpapers/54>

Research Online is the open access institutional repository for the University of Wollongong. For further information contact the UOW Library: [research-pubs@uow.edu.au](mailto:research-pubs@uow.edu.au)

---

## Fabrication and superconducting properties of highly dense MgB<sub>2</sub> bulk using a two-step sintering method

### Abstract

We investigated on microstructure and superconducting properties of high-density MgB<sub>2</sub> superconductors synthesized by a heat-treatment method combining a short period of sintering at 1100 °C with a following annealing at a low temperature. The two-step sintering method was found to achieve a coexistence of a high density and broadened XRD full width at half maximum (FWHM) of MgB<sub>2</sub> peak in the samples. The onset of diamagnetism at 5 T was approximately 2 K higher than those of the samples heat-treated by single-step sintering at high or low temperatures. Different second-step annealing temperatures were examined in this work. Microstructural analysis indicates that a lower second-step annealing temperature led to further suppression of the large grain growth in the MgB<sub>2</sub> samples, which is beneficial to the pinning property of the samples. The energy loss peaks of ac susceptibility measurement in fields confirm that by decreasing the second-step sintering temperature flux pinning of MgB<sub>2</sub> in high fields was enhanced.

### Keywords

Fabrication, superconducting, properties, highly, dense, MgB<sub>2</sub>, bulk, using, two, step, sintering, method

### Disciplines

Engineering | Physical Sciences and Mathematics

### Publication Details

Maeda, M, Zhao, Y, Watanabe, Y, Matsuoka, H & Kubota, Y (2009), Fabrication and superconducting properties of highly dense MgB<sub>2</sub> bulk using a two-step sintering method, IEEE Transactions on Applied Superconductivity, 19(3), pp. 2763-2766.

# Fabrication and Superconducting Properties of Highly Dense $\text{MgB}_2$ Bulk Using a Two-Step Sintering Method

Minoru Maeda, Yue Zhao, Yoshifumi Watanabe, Hiroaki Matsuoka, and Yoji Kubota

**Abstract**—We investigated on microstructure and superconducting properties of high-density  $\text{MgB}_2$  superconductors synthesized by a heat-treatment method combining a short period of sintering at  $1100^\circ\text{C}$  with a following annealing at a low temperature. The two-step sintering method was found to achieve a coexistence of a high density and broadened XRD full width at half maximum (FWHM) of  $\text{MgB}_2$  peak in the samples. The onset of diamagnetism at 5 T was approximately 2 K higher than those of the samples heat-treated by single-step sintering at high or low temperatures. Different second-step annealing temperatures were examined in this work. Microstructural analysis indicates that a lower second-step annealing temperature led to further suppression of the large grain growth in the  $\text{MgB}_2$  samples, which is beneficial to the pinning property of the samples. The energy loss peaks of ac susceptibility measurement in fields confirm that by decreasing the second-step sintering temperature flux pinning of  $\text{MgB}_2$  in high fields was enhanced.

**Index Terms**—Disorder, flux pinning, heat-treatment, high-density ac susceptibility, magnesium diboride.

## I. INTRODUCTION

**S**UPERCONDUCTING material of  $\text{MgB}_2$  has been studied by a lot of researchers owing to real applications, for example, magnets for magnetic resonance imaging and nuclear magnetic resonance.  $\text{MgB}_2$  shows a high critical temperature  $\sim 39$  K compared with Nb-based superconductors [1] and is expected to function as an alternative material in the operating temperature range 10–20 K. However, the  $\text{MgB}_2$  bulks and wires prepared by an *in situ* reaction process are prone to have porosity, which leads to a reduced current-carrying area and low critical current density ( $J_c$ ) in these materials [2], [3]. Decreasing the porosity is essential for  $\text{MgB}_2$  materials to further improve the superconducting properties.  $\text{MgB}_2$  bulks and wires with high densities have been fabricated by several techniques [4]–[7]. High pressure apparatuses are able to manufacture high dense  $\text{MgB}_2$  materials. The densities of the  $\text{MgB}_2$  bulk [4] and

the core of the  $\text{MgB}_2$  tape [5] are respectively  $\sim 2.56 \text{ g/cm}^3$  and  $\sim 2.55 \text{ g/cm}^3$ , close to the theoretical density of  $\text{MgB}_2$  ( $2.625 \text{ g/cm}^3$ ). However, these methods, even if feasible, are limited in some dimensions of the manufactures, due to the practical difficulty in the use of very large vessels, when high pressures and high temperatures are involved. Mg diffusion methods [6], [7] are able to fabricate high-density bulks and wires without the need of uniaxial-hot-pressing and hot-isostatic-pressing. For the abovementioned methods, although the zero-field  $J_c$  increases, the pinning behavior in high fields is not significantly improved. In previous works [8], we reported a two-step heat-treatment within an *in situ* diffusive reaction method for the preparation of near-fully-dense  $\text{MgB}_2$  bulks that also provides very strong in-field pinning. The two-step process achieved a high level of disorder in the  $\text{MgB}_2$  sample together with high density. Moreover, the in-field  $J_c$  is nearly one order of magnitude higher than that of the samples prepared by single-step sintering. This improvement was mainly attributed to a unique feature of well-connected small grains with a high level of disorder in the  $\text{MgB}_2$  samples created by the two-step sintering. In this work, we explore further detailed influence of a two-step sintering method on superconducting properties of  $\text{MgB}_2$ . From the relationship between the full-width-half-maximum (FWHM) of the XRD peaks and the density, we clearly show that the two properties are simultaneously controlled by sintering conditions. We also find that the  $\text{MgB}_2$  sample prepared by a two-step sintering process exhibits better pinning performance in fields than other samples. From the imaginary component of ac susceptibility, we show that the energy loss peak forms various shapes due to two kinds of superconducting phase. Finally, we demonstrate that a lower second-step annealing temperature leads to the improvement of superconducting properties in  $\text{MgB}_2$  due to suppression in an overly large grain growth and a high level of disorder.

## II. EXPERIMENTAL

The polycrystalline  $\text{MgB}_2$  bulks were prepared from Mg lumps (purity 99.99%, size 2–5 mm) and amorphous B powder (99.995%,  $\sim 0.25 \mu\text{m}$ ). The B powder was pressed into slabs with dimensions of  $4.5 \times 21.5 \times 0.5 \text{ mm}$  under a pressure of 100 MPa. The slabs and Mg lumps were placed in a Ta tube 50 mm in length and 6 mm in diameter. The tube was then arc-welded at both ends in a glove box filled with high purity Ar gas. While welding, the Ta tube was heat-sunk with ice-cooled copper block to avoid heating the slabs and Mg lumps. Subsequently the Ta tube was vacuum-sealed in a quartz tube ready

Manuscript received August 26, 2008. First published June 05, 2009; current version published July 15, 2009. This work was supported in part by the U.S. Department of Commerce Grant BS123456.

M. Maeda and Y. Zhao are with the Institute for Superconducting and Electronic Materials, University of Wollongong, Wollongong, NSW 2522, Australia (e-mail: mm723@uow.edu.au; yue@uow.edu.au).

Y. Watanabe, H. Matsuoka, and Y. Kubota are with the College of Science and Technology, Nihon-University, Kanda-Surugadai 1-8-14, Chiyoda-ku, Tokyo, Japan (e-mail: yw4423@yahoo.co.jp; yiu60657@yahoo.co.jp; ykubota@shotgun.phys.cst.nihon-u.ac.jp).

Digital Object Identifier 10.1109/TASC.2009.2017699

TABLE I  
SINTERING CONDITIONS OF THE  $\text{MgB}_2$  SAMPLES

Group	Sample	Heat-treatment1 ( $^{\circ}\text{C} \times \text{h}$ )	Heat-treatment2 ( $^{\circ}\text{C} \times \text{h}$ )	$J_c$ at 3.5T, 20K ( $\text{kA}/\text{cm}^2$ )
H	H0	$1100 \times 0.5$		1.4
	H1	$1100 \times 1$		1.9
	H2	$1100 \times 3$		0.3
L	L0	$660 \times 24$		2.3
	L1	$660 \times 48$		2.8
	L2	$660 \times 96$		2.2
HL	HL0	$1100 \times 0.1$	$660 \times 3$	2.5
	HL1	$1100 \times 0.1$	$660 \times 6$	14.6
	HL2	$1100 \times 0.1$	$660 \times 12$	13.9
LH	LH0	$660 \times 12$	$1100 \times 0.25$	0.01
	LH1	$660 \times 12$	$1100 \times 0.5$	0.01
HL-D	HL-D0	$1100 \times 0.1$	$770 \times 6$	14.3
	HL-D1	$1100 \times 0.1$	$550 \times 192$	32.6

for the following heat-treatments. The starting Mg:B atomic ratio was chosen to be 1:1. Table I summarizes the sintering conditions of the samples. After the heat treatment, the Ta tube was pierced through and again vacuum-sealed in a quartz tube to undergo an Mg evaporation process at  $680^{\circ}\text{C}$  for 0.5 h for removing excess Mg from samples [8]. The phase composition was investigated from XRD patterns which were collected with a Rigaku RINT 2000 diffractometer using  $\text{CuK}\alpha$  radiation. The morphology of the samples was investigated using a HITACHI S-4500 Scanning Electron Microscopy (SEM). A SQUID magnetometer (MPMS-5T, Quantum Design) was used to record the real and the imaginary component curves of ac susceptibility and the dc magnetization loops. The  $T_c$  was determined by ac susceptibility measurements at  $f = 76.97 \text{ Hz}$  with  $\mu_0 H_{ac} = 10 \mu\text{T}$ , and the  $J_c$  values were derived from the magnetization hysteresis loops using the Bean critical state model.

### III. RESULTS AND DISCUSSION

The relation between the FWHM of the  $\text{MgB}_2$  (112) peak and the density for the four types of samples is shown in Fig. 1. The densities for H0, H1, and H2 are  $\sim 2.2$ ,  $\sim 2.4$  and  $\sim 1.9 \text{ g}/\text{cm}^3$  respectively. Noteworthy is that H1 shows a density of  $\sim 90\%$  of theoretical. Nevertheless, the density rapidly decreases with increasing the sintering time from 1 hour to 3 hours. This is believed to be due to a rapid grain growth caused by the excess Mg liquid or vapor at the high temperature in the enough reaction time. The growth was observed by using SEM. Also, Du *et al.* reported that single crystals of  $\text{MgB}_2$  were grown at ambient pressure by evaporating Mg-flux method [9], [10]. The decrease of the density in  $\text{MgB}_2$  causes not only reduced current-carrying areas [2], [3] but also large grains which lead to poor pinning in field [11], [12]. The values of FWHM for Group H were observed to be  $\sim 0.3$  degree, reflecting good crystallized grains of  $\text{MgB}_2$  [8]. The single-step sintering processes at  $1100^{\circ}\text{C}$  are found to synthesize the high density  $\text{MgB}_2$  samples with

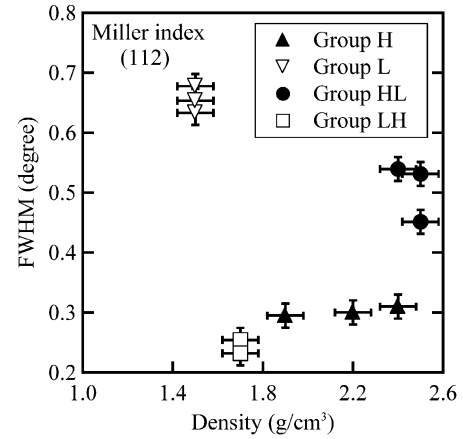


Fig. 1. The relation between the FWHM of the  $\text{MgB}_2$  (112) peak and the density for Group H, L, HL, and LH.

good crystallinity. However, the reaction has the disadvantage of decreasing the density when the long reaction time was used. For Group L, the densities were obtained to be the low values ( $\sim 1.5 \text{ g}/\text{cm}^3$ ) compared with those of Group H, whereas the values of FWHM were observed to be  $\sim 2.2$  times broader than those of Group H. Yamamoto *et al.* reported that the poor crystallinity of  $\text{MgB}_2$  detected from the broadened FWHM contributes to  $H_{C2}$  and  $H_{irr}$  at high field [13]. The single-step sintering carried out at  $660^{\circ}\text{C}$  is found to provide a high level of disorder to the  $\text{MgB}_2$  samples, although the densities for the samples are quite low. In addition, Kim *et al.* reported the effects of sintering conditions on wires fabricated by an *in situ* powder-in-tube (PIT) method [14]. They found the FWHM was significantly broadened by decrease of sintering temperature, whereas the density was slightly changed with increasing sintering temperature on their wire samples.

For Group HL, the densities were showed to be  $\sim 2.4 - 2.5 \text{ g}/\text{cm}^3$  which are comparable to the value of H1. Also, the values of FWHM were observed to be  $\sim 0.53$  degree (HL0 and HL1) and  $\sim 0.45$  degree (HL2) which are broader than those of Group H. Notice that Group HL coexists both of the high density and the broad FWHM. This is because the initial short heat-treatment at  $1100^{\circ}\text{C}$  is too short for an overly large grain growth and complete diffusion. Thanks to the subsequent heat-treatment at  $660^{\circ}\text{C}$  for homogenization, the two-step HL sintering processes achieve a high level of disorder in the  $\text{MgB}_2$  samples together with high density. For Group LH, the densities were showed to be  $\sim 1.7 \text{ g}/\text{cm}^3$  near those of L series. Also, the values of FWHM were observed to be  $\sim 0.24$  degree and the narrowest of all samples. The two-step LH sintering processes synthesize the low dense  $\text{MgB}_2$  samples with good crystallized grains. Accordingly both of the density and the FWHM on  $\text{MgB}_2$  bulks can be simultaneously controlled by the two-step heat-treatments.

Fig. 2 shows the real component of the ac susceptibility for H1, L1, HL1, and LH1, which had the highest  $J_c$  values in Group H, L, HL, and LH respectively. The  $J_c$  values at 20 K in 3.5 T for the four types of samples are listed in Table I. The most noticeable feature shown in this figure is that the onset of diamagnetism at 5 T for HL1 is higher than those of H1 and

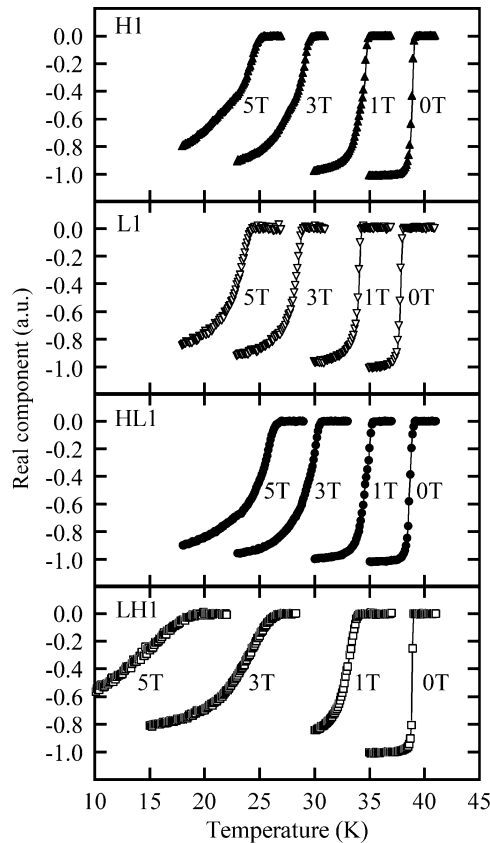


Fig. 2. The real component of the ac susceptibility, with  $f = 76.97$  Hz and  $\mu_0 H_{ac} = 10 \mu\text{T}$  at  $\mu_0 H_{dc} = 0, 1, 3$ , and  $5$  T for H1, L1, HL1, and LH1.

L1 by approximately 2 K. This results from the coexistence of the high density and the high level of disorder in HL1. Also, it should be noted that the onset of diamagnetism at 0 T for H1 is higher than that of L1 by about 1 K, whereas the onset of diamagnetism at 5 T and the  $J_c$  at 20 K for H1 are rather close to those for L1. This is because the level of disorder in L1 is higher than that in H1. The superconducting transitions in fields for LH1 shifted to low temperatures very probably due to the low density and the good crystallinity.

To control the grain size and obtain the high density and the high level of disorder for Group HL, we employed different second sintering conditions. Fig. 3 shows SEM images of surfaces for H1 and the samples which were heat-treated under different second-step temperatures. The surface of H1 in Fig. 3(a) was observed to be large overgrown grains in a dense matrix. By contrast, small grains were seen in the sample heat-treated at  $1100^\circ\text{C} - 0.1 \text{ h} + 550^\circ\text{C} - 192 \text{ h}$  in Fig. 3(d). It also became clear that a lower second-step annealing temperature prevents the large grain growth more effectively, as shown in Figs. 3(b), 3(c), and 3(d). Wang *et al.* reported that the increase of grain size can lead to a decrease of  $J_c$  as a smaller grain size is more beneficial for the enhancement of the grain boundary pinning [12]. The control of the grain size hints at enhanced pinning in the samples heat-treated at  $1100^\circ\text{C} - 0.1 \text{ h} + 550^\circ\text{C} - 192 \text{ h}$ .

Fig. 4 shows the imaginary component of ac susceptibility for H1 and the samples which were heat-treated under

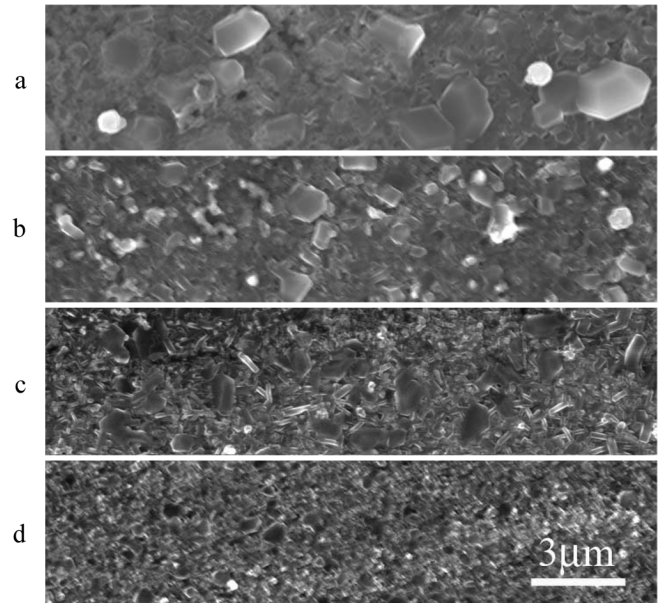


Fig. 3. SEM images of surfaces for samples heat-treated at (a)  $1100^\circ\text{C} - 1 \text{ h}$ , (b)  $1100^\circ\text{C} - 0.1 \text{ h} + 770^\circ\text{C} - 6 \text{ h}$ , (c)  $1100^\circ\text{C} - 0.1 \text{ h} + 660^\circ\text{C} - 6 \text{ h}$ , and (d)  $1100^\circ\text{C} - 0.1 \text{ h} + 550^\circ\text{C} - 192 \text{ h}$ .

different second-step temperatures. H1 exhibits no peak separation with the increasing applied dc field from 0 to 5 T due to the single-step sintering [8], whereas the samples heat-treated by different second sintering conditions show some shoulders in the transition regions. Specifically, in the sample heat-treated at  $1100^\circ\text{C} - 0.1 \text{ h} + 770^\circ\text{C} - 6 \text{ h}$ , the separated peak were observed at 5 T. In the samples heat-treated at  $1100^\circ\text{C} - 0.1 \text{ h} + 550^\circ\text{C} - 192 \text{ h}$  and  $1100^\circ\text{C} - 0.1 \text{ h} + 660^\circ\text{C} - 6 \text{ h}$ , the peak separation started to appear at 0 T and 1 T respectively. These energy loss peak separations suggest that the samples synthesized by the two-step sintering processes consist of two kinds of superconducting phase [8].

The curve of the energy loss peak for the sample heat-treated at  $1100^\circ\text{C} - 0.1 \text{ h} + 550^\circ\text{C} - 192 \text{ h}$ , as shown in Fig. 4(d), shows some interesting behavior. One phase has good ordering of  $\text{MgB}_2$  and generated the peak at higher measured temperature in 0 T indicated by arrow 1. As applied field gradually increased to 1 T, the peak began to disappear. The energy loss peak at 1 T was observed to be a single peak. The reason is that at 1 T the pinning property of the ordered phase is similar to that of the other phase which was believed to have a lower level of ordering and gave rise to the peak at lower measured temperature in 0 T indicated by arrow 2. With increasing applied field from 3 to 5 T, the shoulder appeared in the energy loss peak. The weaker peak marked by arrow 3 is generated by the phase with good ordering of  $\text{MgB}_2$ , indicating comparatively weak pinning. In contrast, the sharper peak indicated by arrow 4 in applied field from 3 or 5 T was believed to possess better pinning which is resulted from a lower level of ordering. Hence, two kinds of superconducting phase form various shapes of the energy loss peaks in fields.

At 0 T, for the curves of ac susceptibility of the samples heat-treated under different second-step temperatures, a lower

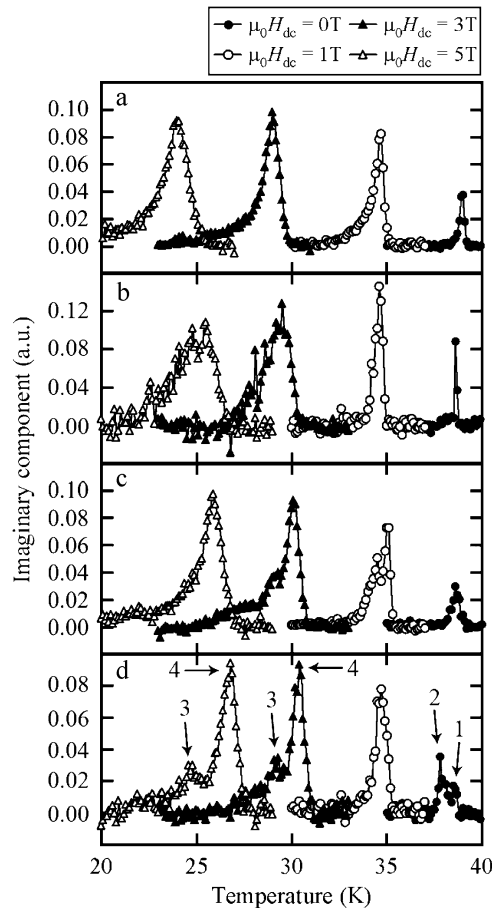


Fig. 4. The imaginary component of the ac susceptibility, with  $f = 76.97$  Hz and  $\mu_0 H_{ac} = 10 \mu T$  at  $\mu_0 H_{dc} = 0, 1, 3$ , and  $5$  T for (a)  $1100^\circ C - 1$  h, (b)  $1100^\circ C - 0.1$  h +  $770^\circ C - 6$  h, (c)  $1100^\circ C - 0.1$  h +  $660^\circ C - 6$  h, and (d)  $1100^\circ C - 0.1$  h +  $550^\circ C - 192$  h.

second-step annealing temperature caused not only a slight shift to a lower measured temperature but also a peak separation. The reason is because a lower sintering temperature tends to achieve poorer crystallinity in the  $MgB_2$  samples [14]. It also should be noted that the energy loss peak at  $5$  T shifts to higher temperatures with decreasing second-step annealing temperature. This is attributed to both of smaller grains and a lower level of ordering. Therefore, decreasing second-step sintering temperature results in an improvement of the pinning property at high field.

#### IV. SUMMARY

In this work, we have studied superconducting properties of highly dense  $MgB_2$  bulk using a two-step sintering method. This technique effectively controls the grain size and the level of

disorder while achieving high density in the  $MgB_2$  samples. The samples show two kinds of superconducting phase, reflecting a peak separation on the imaginary component of ac susceptibility in field. Finally, we have demonstrated that a lower second-step sintering temperature improves the pinning property of  $MgB_2$ .

#### ACKNOWLEDGMENT

The authors thank Professor Shi Xue Dou, the Institute for Superconducting and Electronic Materials, University of Wollongong, Australia, for helpful discussions.

#### REFERENCES

- [1] J. Nagamatsu, N. Nakagawa, T. Muranaka, Y. Zenitani, and J. Akimitsu, "Superconductivity at  $39$  K in magnesium diboride," *Nature*, vol. 410, pp. 63–64, Mar. 2001.
- [2] C. F. Liu, G. Yan, S. J. Du, W. Xi, Y. Feng, P. X. Zhang, X. Z. Wu, and L. Zhou, "Effect of heat-treatment temperatures on density and porosity in  $MgB_2$  superconductor," *Physica C*, vol. 386, pp. 603–606, Apr. 2003.
- [3] S. Jin, H. Mavoori, C. Bower, and R. B. van Dover, "High critical currents in iron-clad superconducting  $MgB_2$  wires," *Nature*, vol. 411, pp. 563–565, May 2001.
- [4] A. T. Findikoglu, A. Serquis, L. Cival, X. Z. Liao, Y. T. Zhu, M. E. Hawley, F. M. Mueller, V. F. Nesterenko, and Y. Gu, "Microwave performance of high-density bulk  $MgB_2$ ," *Appl. Phys. Lett.*, vol. 83, pp. 108–110, Jul. 2003.
- [5] H. Fang, Y. Y. Xue, Y. X. Zhou, A. Baikalov, and K. Salama, "Densification of  $MgB_2$  cores in iron-clad tapes," *Supercond. Sci. Technol.*, vol. 17, pp. L27–L29, Jul. 2004.
- [6] G. Giunchi, "High density  $MgB_2$  obtained by reactive liquid Mg infiltration," *Int. J. Mod. Phys.*, vol. 17, pp. 453–460, Mar. 2003.
- [7] S. Ueda, J. Shimoyama, I. Iwayama, A. Yamamoto, Y. Katsura, S. Horii, and K. Kishio, "High critical current properties of  $MgB_2$  bulks prepared by a diffusion method," *Appl. Phys. Lett.*, vol. 86, no. 222502, May 2005.
- [8] M. Maeda, Y. Zhao, S. X. Dou, Y. Nakayama, T. Kawakami, H. Kobayashi, and Y. Kubota, "Fabrication of highly dense  $MgB_2$  bulk at ambient pressure," *Supercond. Sci. Technol.*, vol. 21, no. 032004, Mar. 2008.
- [9] W. Du, H. Xu, H. Zhang, D. Xu, X. Wang, X. Hou, Y. Wu, F. Jiang, and L. Qin, "Single crystal growth of  $MgB_2$  by evaporating Mg-flux method," *J. Crystal Growth*, vol. 289, pp. 626–629, Apr. 2006.
- [10] W. Du, D. Xu, H. Zhang, X. Wang, G. Zhang, X. Hou, H. Liu, and Y. Wang, "Single crystal growth of  $MgB_2$  by using Mg-self-flux method at ambient pressure," *J. Crystal Growth*, vol. 268, pp. 123–127, Jul. 2004.
- [11] P. Mikheenko, E. Martinez, A. Bevan, J. S. Abell, and J. L. MacManus-Driscoll, "Grain boundaries and pinning in bulk  $MgB_2$ ," *Supercond. Sci. Technol.*, vol. 20, pp. S264–S270, Sep. 2007.
- [12] S. F. Wang, Z. Liu, Y. L. Zhou, Y. B. Zhu, Z. H. Chen, H. B. Lu, B. L. Cheng, and G. Z. Yang, "Correlation between film thickness and critical current density of  $MgB_2$  films," *Supercond. Sci. Technol.*, vol. 17, pp. 1126–1128, Oct. 2007.
- [13] A. Yamamoto, J. Shimoyama, S. Ueda, Y. Katsura, S. Horii, and K. Kishio, "Improved critical current properties observed in  $MgB_2$  bulks synthesized by low-temperature solid-state reaction," *Supercond. Sci. Technol.*, vol. 18, pp. 116–121, Jan. 2005.
- [14] J. H. Kim, S. X. Dou, D. Q. Shi, M. Rindfleisch, and M. Tomsic, "Study of  $MgO$  formation and structural defects in *in situ* processed  $MgB_2$ /Fe wires," *Supercond. Sci. Technol.*, vol. 20, pp. 1026–1031, Oct. 2007.